On the Temperature and Pressure Dependence of a Range of Properties of a Type of Water Model Commonly Used in High-Temperature Protein Unfolding Simulations

Regula Walser, Alan E. Mark, and Wilfred F. van Gunsteren
Laboratory of Physical Chemistry, Swiss Federal Institute of Technology Zürich, CH-8092 Zürich, Switzerland

ABSTRACT Molecular dynamics simulations of protein folding and unfolding are often carried out at temperatures (400–600 K) that are much higher than physiological or room temperature to speed up the (un)folding process. Use of such high temperatures changes both the protein and solvent properties considerably, compared to physiological or room temperature. Water models designed for use in conjunction with biomolecules, such as the simple point charge (SPC) model, have generally been calibrated at room temperature and pressure. To determine the distortive effect of high simulation temperatures on the behavior of such "room temperature" water models, the structural, dynamic, and thermodynamic properties of the much-used SPC water model are investigated in the temperature range from 300 to 500 K. Both constant pressure and constant volume conditions, as used in protein simulations, were analyzed. We found that all properties analyzed change markedly with increasing temperature, but no phase transition in this temperature range was observed.

INTRODUCTION

Molecular dynamics simulations are widely used to gain insight into the equilibrium properties of proteins in solution. Increasingly, simulations are also being used to study time- and environment-dependent phenomena, such as the folding or unfolding of proteins. In particular, many simulations of the process of thermal denaturation have been performed. Currently accessible time scales of $\sim 10^{-9}$ s are insufficient, however, to simulate folding and unfolding processes at experimentally relevant temperatures. To circumvent this problem most simulations of protein unfolding have used high simulation temperatures to shorten the time scale of the unfolding process. For example, the thermal unfolding of hen egg white (HEW) lysozyme in water was simulated at 500 K (Mark and van Gunsteren, 1992). The destabilization of bovine pancreatic trypsin inhibitor (BPTI) and its reduced form in water was simulated at 423 K and 498 K (Daggett and Levitt, 1992, 1993). The denaturation of the C-terminal fragment (CTF) of the L7/L12 ribosomal protein was simulated at 498 K (Daggett, 1993), that of the enzyme β-lactamase at 600 K (Vijayakumar et al., 1993), and that of the protein barnase at 498 K and 600 K (Caflisch and Karplus, 1994, 1995; Li and Daggett, 1998; Bond et al., 1997). Potato carboxypeptidase inhibitor was simulated at 600 K (Martì-Renom et al., 1998), and cutinase was simulated at 393 K (Creveld et al., 1998).

In each of these cases the proteins unfold. The question is, how relevant are the results from a simulation of a protein at 500 K to the process of thermal denaturation close to physiological temperatures? At a more basic level one must also ask if the molecular models and simulation protocols developed for use at 300 K are still appropriate at elevated temperatures.

The process of protein folding and unfolding is driven by the balance between protein-protein, protein-water, and water-water interactions. Each of these interactions involves some degree of enthalpy-entropy compensation and will depend on the temperature. At nonphysiological temperatures the unfolding pathways may also be quite different from that at 300 K. For one, at high temperature the structural, dynamic, and thermodynamic properties of a solvent such as water will differ from those at 300 K, which will in turn affect the process of protein unfolding.

In this paper we investigate the extent to which the structural, dynamic, and thermodynamic properties of a water model commonly used in biomolecular simulations, the simple point charge (SPC) model (Berendsen et al., 1981), change as a function of temperature between 300 and 500 K.

Because protein unfolding simulations at high temperatures have been carried out at constant volume as well as at constant pressure, the properties of liquid water are investigated under both these conditions.

Other studies of the temperature dependence of the properties of water have been published. However, these studies have not covered the whole range of temperatures or properties relevant to protein destabilization and denaturation simulations. They have either focused on the range up to 373 K (Jorgensen and Jenson, 1998), on the phase equilibrium (Boulougouris et al., 1998; de Pablo et al., 1990), or on the supercritical conditions (Jedlovszky et al., 1998; Jedlovszky and Richardi, 1999; Bursulaya and Kim, 1999a,b),

Received for publication 15 November 1999 and in final form 13 March 2000.

Address reprint requests to Prof. Wilfred F. van Gunsteren, Laboratory of Physical Chemistry, ETH-Zürich, CH-8092 Zürich, Switzerland. Tel: +41-1-6325502; Fax: +41-1-6321039; E-mail: wfvgn@igc.phys.chem.ethz.ch.

The present address of Prof. Mark is Laboratory of Biophysical Chemistry, University of Groningen, Nijenborgh 4, 9747 AG Groningen, the Netherlands.

0006-3495/00/06/2752/09 $2.00

or considered only a limited set of properties. When Levitt et al. (1997) developed and tested their flexible water model F3C, they also examined some of its properties, i.e., energy, heat capacity, radial distribution function, and diffusion constant at higher temperatures. Brodholt and Wood (1993) investigated the behavior of the energy, pressure, heat capacity, and radial distribution function of TIP4P (Jorgensen et al., 1983) as well as SPC/E (Berendsen et al., 1987) and a model by Watanabe and Klein (1989) over a wide temperature range (up to 2600 K). However, none of these studies looked at the free energy and dynamical properties of water, which also might affect protein (un)folding. Here we concentrate in particular on those properties of water that may influence the process of protein unfolding and lead to artifacts in unfolding simulations.

Method

Simulation

At five temperatures, 300, 350, 400, 450, and 500 K, two simulations were performed, one at constant pressure and one at constant volume. The system consisted of a cubic periodic box containing 1000 SPC water molecules (Berendsen et al., 1981). Bond lengths and angles were constrained using the SHAKE algorithm (Ryckaert et al., 1977), with a relative tolerance of 10^{-4}. The system was equilibrated for 50 ps at each temperature and then simulated for 250 ps for analysis. Configurations 0.05 ps apart were saved. The temperature was kept constant by a Berendsen thermostat (Berendsen et al., 1984) (weak coupling) with a coupling time of 0.1 ps. In the constant-pressure simulations the pressure was kept at 1 atm by weak coupling to an external bath (Berendsen et al., 1984) with a relaxation time of 0.5 ps and a compressibility of 7.5×10^{-4}mol nm^3/kJ. In the constant-volume simulations the volume was fixed at 29.9151 nm^3 (box length of 3.1043 nm), which corresponds to a density of 602.22 u/nm^3 (1.0 g/cm^3). All simulations were performed using the GROMOS96 simulation package (van Gunsteren et al., 1996; Scott et al., 1999) with a time step of 2 fs. The nonbonded interactions were calculated using a twin cutoff of 0.9 nm/1.4 nm for the oxygen-oxygen distances. The interaction between water molecules with oxygen-oxygen distances between 0.9 nm and 1.4 nm were updated every 10 fs. No reaction-field correction to long-range electrostatic interactions was applied.

The excess free energy ΔA_{exs} of the water model at each temperature was determined using the thermodynamic integration method. The volume was kept constant. All intermolecular interactions were scaled as a function of the coupling parameter λ (Daura et al., 1996). Simulations were performed at 29 λ points between $\lambda = 0$ and $\lambda = 1$. At each λ-point 20 ps for equilibration and 50 ps for analysis were calculated.

The hydration free enthalpy ΔG_{hyd} was calculated in the same way, except that the pressure was kept constant and the intermolecular interactions of only one molecule were scaled as a function of the coupling parameter.

Analysis

The presence of a hydrogen bond was determined based on a geometric criterion. If the O—H distance was less then 0.25 nm and the O-H—O angle greater than 135°, a hydrogen bond was considered to exist between the two water molecules. The diffusion constant was estimated from the Einstein formula,

$$D = \lim_{t\to\infty} \frac{\langle (\mathbf{r}(t) - \mathbf{r}(0))^2 \rangle}{6t}, \tag{1}$$

where $\mathbf{r}(t)$ is the position vector of a molecule's center of mass at time t. The thermal expansion coefficients α have always been calculated from two simulations at constant pressure with $\Delta T = 50$ K via (Tironi and van Gunsteren, 1994)

$$\alpha \approx -\left(\frac{\ln(\rho_2/\rho_1)}{T_2 - T_1}\right)_{\mathrm{p}}, \tag{2}$$

in which ρ_1 and ρ_2 are the densities at temperatures T_1 and T_2.

The heat capacity C_{p} was calculated using (Postma, 1985)

$$C_{\mathrm{p}} \approx \frac{E_{\mathrm{tot},2} - E_{\mathrm{tot},1}}{T_2 - T_1} + \frac{\partial E_{\mathrm{int}}}{\partial T} + \frac{\partial E_{\mathrm{ext}}}{\partial T}, \tag{3}$$

where E_{int} is the (quantum) contribution of intramolecular vibrational modes to the specific heat. E_{ext} is the difference between the quantum-mechanical and the classical intermolecular vibrational energy. Those corrections have been calculated as described by Postma (1985). At 300 K their combined value is -9.3 J mol^{-1} K^{-1} (Postma, 1985). The rotational correlation times τ_l were calculated by fitting to the linear part in a logarithmic plot of the Legendre polynomial correlation function of rank l, $\langle P_l(\cos\,\theta(t))\rangle$, where $\cos(\theta(t))$ denotes the scalar product of the corresponding dipole vectors of unit length separated by a time t.

RESULTS

Thermodynamic properties

Fig. 1 shows the total energy, the kinetic energy, the potential energy, the van der Waals energy, the electrostatic energy, and the heat of vaporization for the SPC model as a function of temperature. In the simulations with constant pressure the change in the total energy is larger than in the simulations with constant volume, as the computational box is unable to relax in the latter. The heat of vaporization

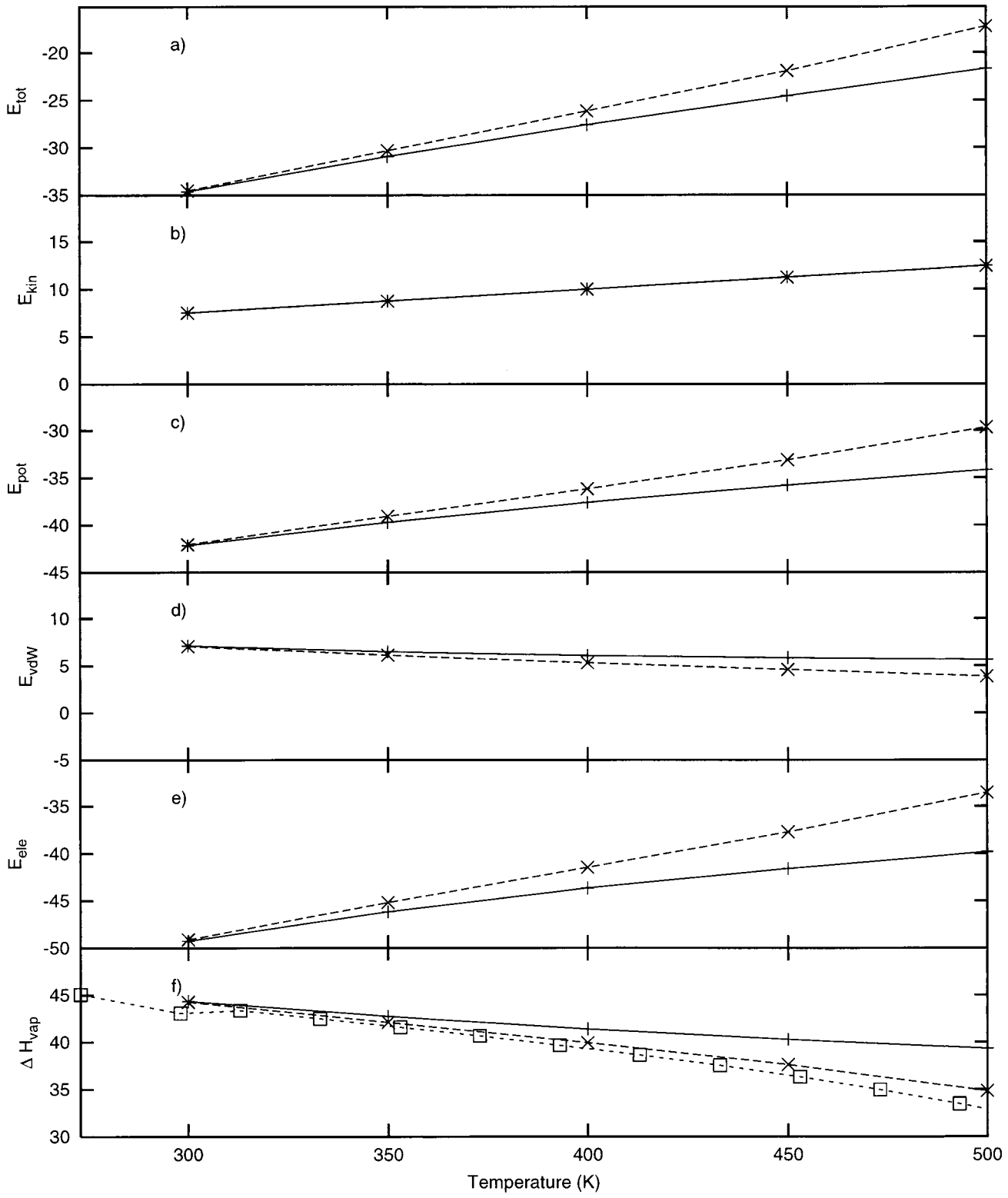

FIGURE 1 The total, kinetic, potential, van der Waals, and electrostatic energies (in kJ/mol) are shown as a function of temperature for the simulations with constant pressure (×, – – –, p = 1 atm = 0.061 kJ/mol/nm^3) and with constant volume (+, ——, ρ = 1.0 g/cm^3 = 602 u/nm^3). All quantities are given per molecule. In *f* the heat of vaporization, calculated with Eq. 4, is compared to the experimental heat of vaporization (□, - - - -) (Marsh, 1987). The lines have been added to guide the eye.

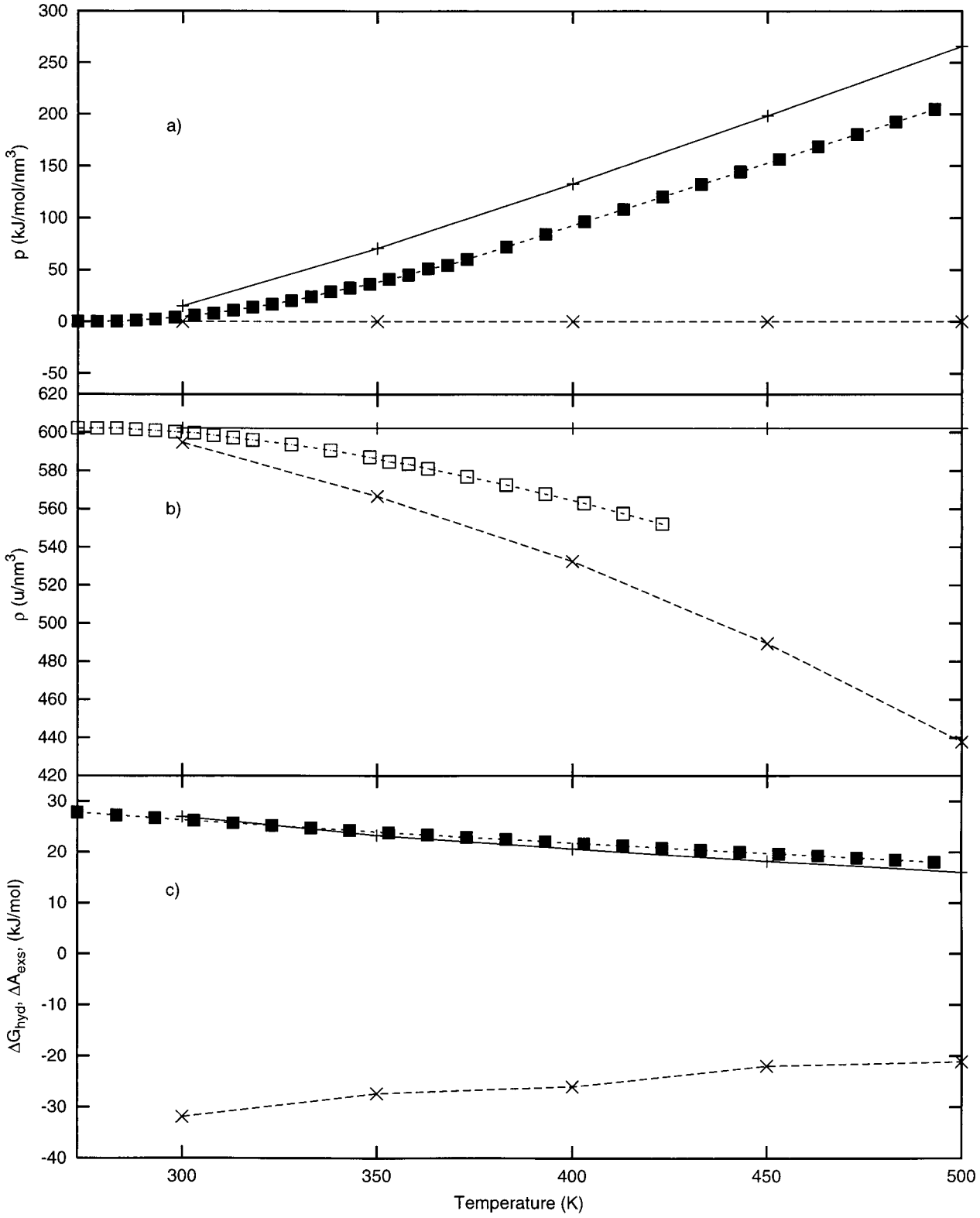

FIGURE 2 Pressure (p), density (ρ), and free energies (ΔG_{hyd} and ΔA_{exs}) are shown as a function of temperature. In *a* the pressure is compared to the experimental pressure of water with density 1.00 g/cm^3 (■, - - - -). The values were taken from Haar et al. (1988). The experimental values for the density were taken from Kell (1967); those above 373 K refer to the metastable liquid. The excess free energy ΔA_{exs} (+, ——) is compared with the experimental values (■, - - - -) calculated as described in the text. ΔG_{hyd} (×, – – –) is the hydration free enthalpy. For further explanation see caption of Fig. 1.

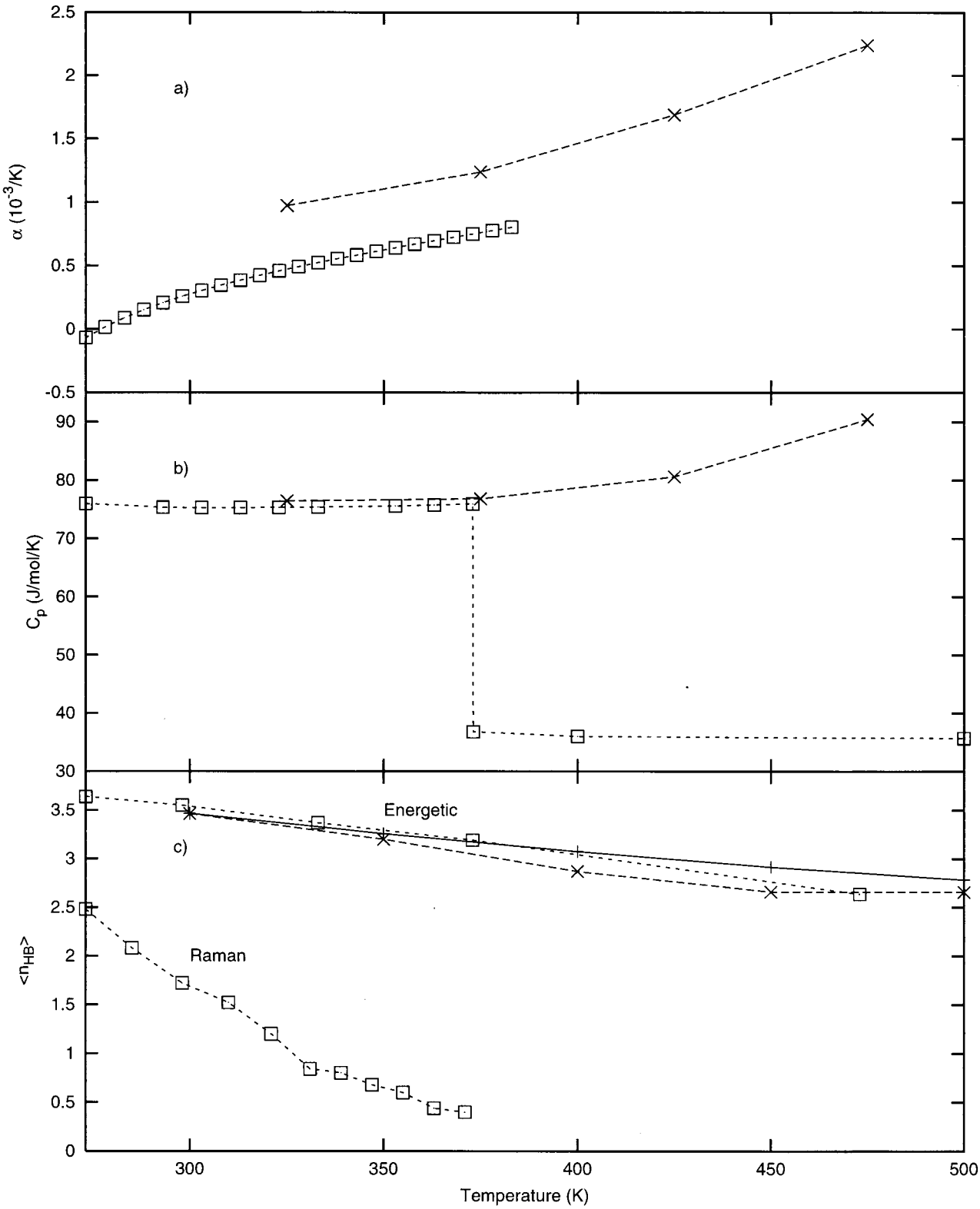

FIGURE 3 Thermal expansion coefficient α and heat capacity C_P were calculated from the simulations at constant pressure with Eqs. 2 and 3. The experimental values for α were taken from Kell (1967). The values above 373 K refer to the metastable liquid at 1 atm. The experimental values for C_P were taken from Weast (1976). The average number of hydrogen bonds per molecule ($\langle n_{HB} \rangle$) is shown as a function of temperature. The hydrogen bond criterion is given in the text. The experimental values obtained by Raman spectroscopy were estimated from the graph in Walrafen (1966); those obtained by energetic considerations were taken from Haggis et al. (1952). For further explanation see caption of Fig. 1.

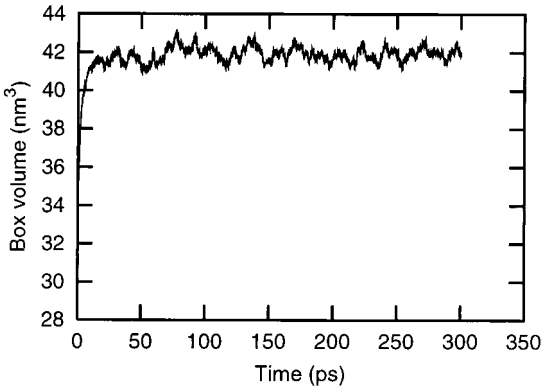

FIGURE 4 Box volume of the simulation at 500 K with constant pressure (1 atm = 0.061 kJ/mol/nm^3) as a function of time.

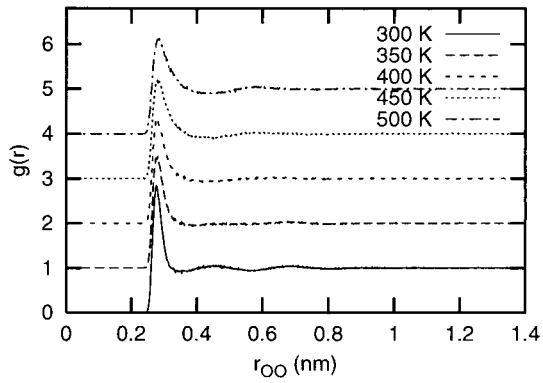

FIGURE 5 Oxygen-oxygen radial distribution function $g(r)$ of the simulations with constant volume (ρ = 1.0 g/cm^3 = 602 u/nm^3) for different temperatures. The different curves are vertically shifted by one unit for better visibility.

ΔH_{vap} is estimated from the simulations as

$$\Delta H_{vap} = -E_{pot} + p\Delta V + Q_{int} + Q_{ext}, \qquad (4)$$

where $p\Delta V$ can be approximated by RT, because ΔV is essentially equal to V_{gas}. Q_{int} is the intramolecular (quantum) contribution for the difference in vibrational energy between the liquid state and the gas phase, and Q_{ext} is its intermolecular counterpart (Postma, 1985). At 300 K, $Q_{int} + Q_{ext} = -0.23$ kJ/mol (Postma, 1985).

Comparing the vaporization enthalpy calculated in this way to the experimental vaporization enthalpy (Marsh, 1987) along the liquid-vapor curve, there is good agreement, although the simulated values are higher than the experimental ones.

The pressures and densities are shown in Fig. 2. The decrease in density as a function of temperature in the constant-pressure simulations is greater than observed experimentally for water up to 373 K. Beyond 373 K, where water is a gas at 1 atm, the simulations clearly overestimate the density. No sudden decrease in density with temperature, which would indicate vaporization, was observed.

The calculated free energies are shown and compared to the experimental values in Fig. 2 *c*. The experimental values of the excess free energy ΔA_{exs} are calculated from the vapor pressure by

$$\Delta A_{exs}(T) \approx RT\left(\ln\left(\frac{RT}{p_{vap}(T)v(T)}\right) - 1\right), \qquad (5)$$

where p_{vap} is the vapor pressure at temperature T and v is the molar volume of water. The values for p_{vap} and v are taken from Schmidt (1989). The calculated excess free energy agrees well with the experimental one over the whole temperature range from 300 to 500 K.

In Fig. 3 *a* the results for the thermal expansion coefficient α are shown. The values are too high compared to the experimental values (Kell, 1967), as can also be seen in Fig. 2 *b*, where the density decreases faster than the experimental density. Although the thermal expansion coefficient is too large, its behavior with increasing temperature is correct, because the slope is about the same as for the experimental values. The heat capacity C_p, shown in Fig. 3 *b*, agrees very well with the experimental values (Weast, 1976) up to 373 K. Above 373 K, the results are noncomparable, as in the simulation the water does not evaporate. Jorgensen and Jenson (1998) calculated C_p and α for SPC at 298 K from the fluctuations of the energy and volume. They obtained values that are slightly higher than the values calculated here, 1.06×10^{-3} K^{-1} (Jorgensen and Jenson, 1998) for α compared to 0.97×10^{-3} K^{-1} and 84.5 J mol^{-1} K^{-1} (Jorgensen and Jenson, 1998) for C_p compared to 76.4 J mol^{-1} K^{-1}.

Structural properties

The number of hydrogen bonds per molecule shown in Fig. 3 *c* decreases almost linearly in the constant-volume simu-

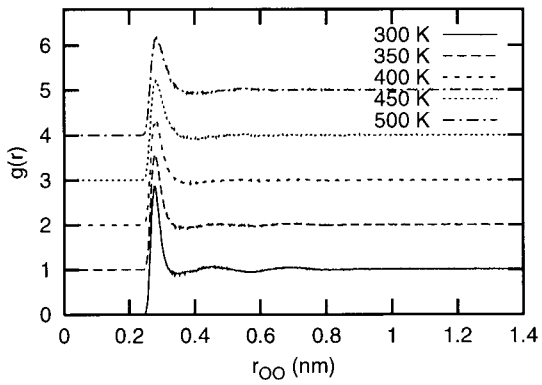

FIGURE 6 Oxygen-oxygen radial distribution function $g(r)$ of the simulations with constant pressure (p = 1 atm = 0.061 kJ/mol/nm^3) for different temperatures. The different curves are vertically shifted by one unit for better visibility.

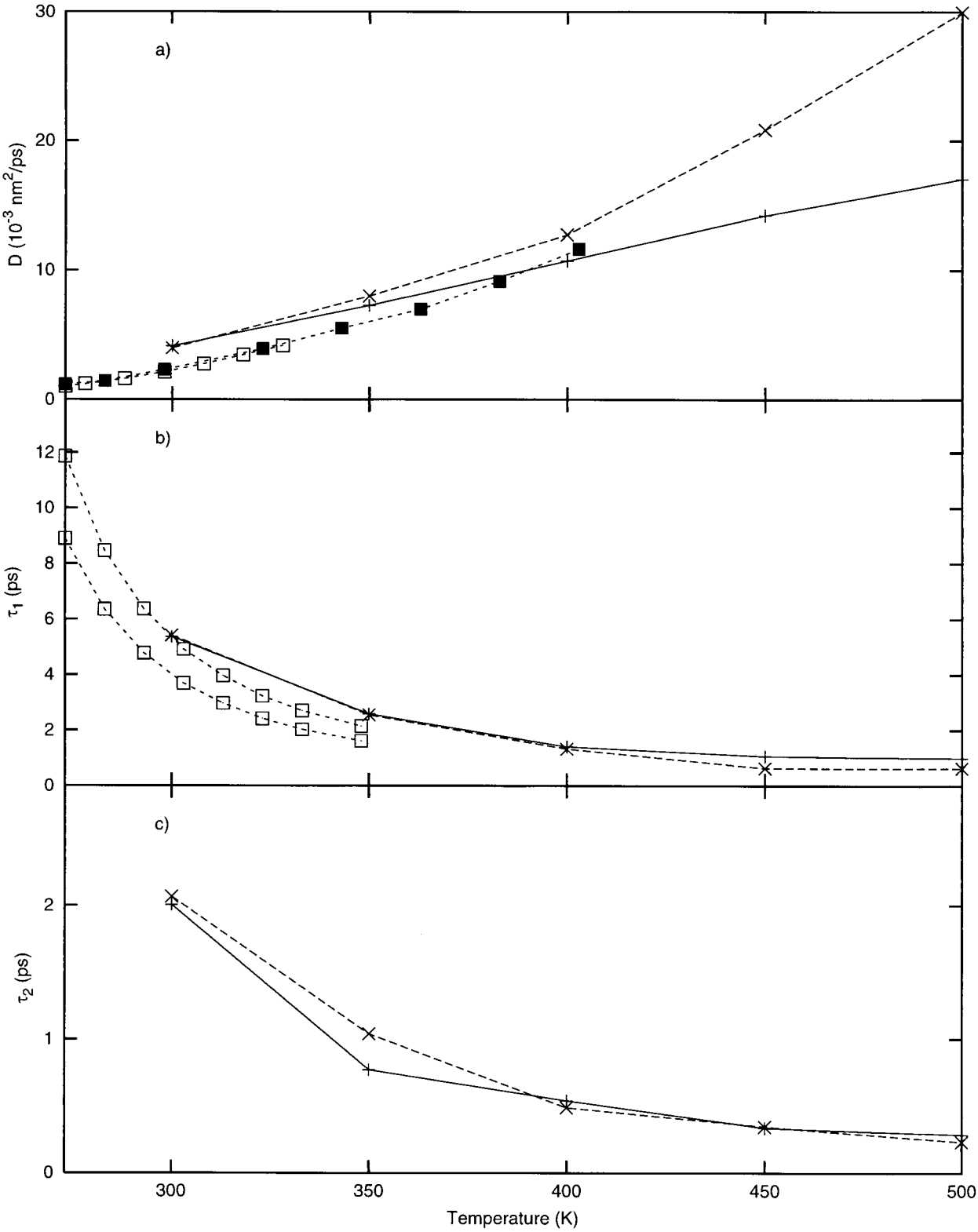

FIGURE 7 The translational diffusion constant (D) and the dipolar rotational correlation times (τ_i) are shown as a function of temperature. The experimental values for D at atmospheric pressure (□) were taken from Becke (1974), those at the pressure corresponding (according to Haar et al., 1988) to a density ρ of 1.0 g/cm^3 (■) were taken from Krynicki (1978). The experimental values for τ_1 correspond to $\frac{2}{3}\tau_D$ and $\frac{1}{2}\tau_D$ as described in the text. Values for τ_D were taken from Collie et al. (1948). For further explanation see caption of Fig. 1.

lations. The value of 3.46 hydrogen bonds per molecule under ambient conditions corresponds well to the results of Jorgensen et al. (1983), who found 3.54 hydrogen bonds per molecule, although they used an energetic definition of a hydrogen bond. The results also agree well with the experimental results of Haggis et al. (1952), who determined the percentage of broken hydrogen bonds by energetic considerations. However, they are completely different from the experimental results of Walrafen (1966), who determined the fraction of hydrogen bonds by Raman spectroscopy. In the constant-pressure simulations the number levels off above 450 K. This could indicate clustering of molecules, but no clustering was observed from visual inspection of specific configurations. The computational box did not expand further after ~20 ps (see Fig. 4), and we found no indication that the liquid would evaporate on a 100-ps time scale.

Figs. 5 and 6 show radial distribution functions $g(r)$ between the oxygen atoms of different molecules at the different temperatures. With constant pressure and with constant volume, the peak height decreases with increasing temperature and the first minimum shifts toward longer distances. The second peak that is visible at 300 K disappears at higher temperatures, but there seems to be a second peak reappearing at 500 K. This agrees somewhat with the results of Brodholt and Wood (1993) for the TIP4P water model, who saw the second peak disappearing at 340 K and reappearing at 771 K.

Dynamic properties

The results for the dynamic properties are shown in Fig. 7. The simulated diffusion coefficient is larger than the experimental one (Becke, 1974; Krynicki et al., 1978) up to ~400 K, but it changes less with increasing temperature than in the experiment. The increase with temperature is stronger for constant-pressure simulations, especially for temperatures above 400 K. The dipolar rotational correlation times τ_l decrease with increasing temperature. There is no significant difference between the constant-pressure and the constant-volume simulations. τ_1 is compared to the experimentally measurable decay time τ_D of the macroscopic polarization (Collie et al., 1948). It should be between $\frac{1}{2}\tau_D$ and $\frac{2}{3}\tau_D$ (Powles, 1953; Nee and Zwanzig, 1970). Although the values at 300 K lie in this range, it looks like τ_1 is not decaying fast enough with temperature compared to experiment. The ratio between τ_1 and τ_2 is for most temperatures between 2.5 and 3, except for constant pressure at 450 K and for constant volume at 500 K, where it is 1.8 and 3.5, respectively. These deviations probably result from the way τ_l is calculated. At high temperatures the exponential part in the decay function is short. Thus few points for fitting are available.

CONCLUSIONS

In an attempt to investigate the behavior of the solvent in simulations at higher temperatures, simulations of SPC water have been performed at temperatures up to 500 K. From the present work, the conclusion is that the structure of the solvent changes with increasing temperature. Although there is no vaporization of the water even at temperatures up to 500 K, the number of hydrogen bonds per molecule decreases. The excess free energy and hydration free enthalpy per water molecule change by ~10 kJ/mol over this temperature range. Both of these factors would be expected to affect the folding of a protein. In addition, the dynamics of the water molecules changes quite dramatically. Of course, all dynamic properties indicate that the molecules move much faster; the diffusion increases by four- (NVT) to sevenfold (NPT) when the temperature is raised from 300 K to 500 K.

In general the properties of the NVT and NPT systems, which are effectively equivalent at 300 K, 1 atm, and a density of 1 g/cm^3, deviate widely with increasing temperature. The choice of ensemble in simulations of proteins at high temperature is thus a critical issue.

Overall, in comparison with the available experimental data, it is apparent that the SPC water model performs well over a wide range of temperature. This said, it is also clear that at elevated temperatures not only does the model begin to deviate from experiment, but the properties of water as a solvent are also very different from those under which thermal denaturation is studied experimentally. The use of temperatures beyond 400 K in simulations of proteins in water is very likely to significantly affect the (un)folding thermodynamics, pathways, and kinetics. Its results should therefore be very cautiously interpreted.

Financial support was obtained from the Schweizerischer Nationalfonds, project number 21-50929.97, which is gratefully acknowledged.

REFERENCES

Becke, M., editor. 1974. Gmelin Handbuch der anorganischen Chemie, 8th Ed. Springer-Verlag, Berlin.

Berendsen, H. J. C., J. R. Grigera, and T. P. Straatsma. 1987. The missing term in effective pair potentials. *J. Phys. Chem.* 91:6269–6271.

Berendsen, H. J. C., J. P. M. Postma, W. F. van Gunsteren, A. DiNola, and J. R. Haak. 1984. Molecular dynamics with coupling to an external bath. *J. Chem. Phys.* 81:3684–3690.

Berendsen, H. J. C., J. P. M. Postma, W. F. van Gunsteren, and J. Hermans. 1981. Interaction models for water in relation to protein hydration. *In* Intermolecular Forces. B. Pullman, editor. Reidel, Dordrecht, the Netherlands. 331–342.

Bond, C. J., K.-B. Wong, J. Clarke, A. R. Fersht, and V. Daggett. 1997. Characterization of residual structure in the thermally denatured state of barnase by simulation and experiment: description of the folding pathway. *Proc. Natl. Acad. Sci. USA.* 94:13409–13413.

Boulougouris, G. C., I. G. Economou, and D. N. Theodorou. 1998. Engineering a molecular model for water phase equilibrium over a wide temperature range. *J. Phys. Chem. B.* 102:1029–1035.

Brodholt, J., and B. Wood. 1993. Simulation of the structure and thermodynamic properties of water at high pressures and temperatures. *J. Geophys. Res.* 98:519–536.

Bursulaya, B. D., and H. J. Kim. 1999a. Molecular dynamics simulation study of water near critical conditions. I. Structure and solvation free energetics. *J. Chem. Phys.* 110:9646–9655.

Bursulaya, B. D., and H. J. Kim. 1999b. Molecular dynamics simulation study of water near critical conditions. II. Dynamics and spectroscopy. *J. Chem. Phys.* 110:9656–9665.

Caflisch, A., and M. Karplus. 1994. Molecular dynamics simulation of protein denaturation: solvation of the hydrophobic cores and secondary structure of barnase. *Proc. Natl. Acad. Sci. USA.* 91:1746–1750.

Caflisch, A., and M. Karplus. 1995. Acid and thermal denaturation of barnase investigated by molecular dynamics simulations. *J. Mol. Biol.* 252:672–708.

Collie, C. H., J. B. Hasted, and D. M. Ritson. 1948. The dielectric properties of water and heavy water. *Proc. Phys. Soc.* 60:145–160.

Creveld, L. D., A. Amadei, R. C. van Schaik, H. A. M. Pepermans, J. de Vlieg, and H. J. C. Berendsen. 1998. Identification of functional and unfolding motions of cutinase as obtained from molecular dynamics computer simulations. *Proteins.* 33:253–264

Daggett, V. 1993. A model for the molten globule state of (CTF) generated using molecular dynamics. *In* Techniques in Protein Chemistry IV. R. H. Angeletti, editor. Academic Press, San Diego. 525–532.

Daggett, V., and M. Levitt. 1992. A model of the molten globule state from molecular dynamics simulations. *Proc. Natl. Acad. Sci. USA.* 89: 5142–5146.

Daggett, V., and M. Levitt. 1993. Protein unfolding pathways explored through molecular dynamics simulations. *J. Mol. Biol.* 232:600–619.

Daura, X., P. H. Hünenberger, A. E. Mark, E. Querol, F. X. Avilés, and W. F. van Gunsteren. 1996. Free energies of transfer of Trp analogs from chloroform to water: comparison of theory and experiment and the importance of adequate treatment of electrostatic and internal interactions. *J. Am. Chem. Soc.* 118:6285–6294.

de Pablo, J. J., J. M. Prausnitz, H. J. Strauch, and P. T. Cummings. 1990. Molecular simulation of water along the liquid-vapor coexistence curve from 25°C to the critical point. *J. Chem. Phys.* 93:7355–7359.

Haar, L., J. S. Gallagher, and G. S. Kell. 1988. NBS)/NRC Wasserdampftafeln. Springer-Verlag, Berlin.

Haggis, G. H., J. B. Hasted, and T. J. Buchanan. 1952. The dielectric properties of water in solutions. *J. Chem. Phys.* 20:1453–1465.

Jedlovszky, P., J. P. Brodholt, F. Bruni, M. A. Ricci, A. K. Soper, and R. Vallauri. 1998. Analysis of the hydrogen-bonded structure of water from ambient to supercritical conditions. *J. Chem. Phys.* 108:8528–8540.

Jedlovszky, P., and J. Richardi. 1999. Comparison of different water models from ambient to supercritical conditions: a Monte Carlo simulation and molecular Ornstein-Zernike study. *J. Chem. Phys.* 110: 8019–8031.

Jorgensen, W. L., J. Chandrasekhar, J. D. Madura, R. W. Impey, and M. L. Klein. 1983. Comparison of simple potential functions for simulating liquid water. *J. Chem. Phys.* 79:926–935.

Jorgensen, W. L., and C. Jenson. 1998. Temperature dependence of TIP3P, SPC, and TIP4P water from NPT Monte Carlo simulations: seeking temperatures of maximum density. *J. Comp. Chem.* 19:1179–1186.

Kell, G. S. 1967. Precise representation of volume properties of water at one atmosphere. *J. Chem. Eng. Data.* 12:66–69.

Krynicki, K., C. D. Green, and D. W. Sawyer. 1978. Pressure and temperature dependence of self-diffusion in water. *Faraday Discuss. Chem. Soc.* 66:199–208.

Levitt, M., M. Hirshberg, R. Sharon, K. E. Laidig, and V. Daggett. 1997. Calibration and testing of a water model for simulation of the molecular dynamics of proteins and nucleic acids in solution. *J. Phys. Chem. B.* 101:5051–5061.

Li, A., and V. Daggett. 1998. Molecular dynamics simulation of the unfolding of barnase: characterization of the major intermediate. *J. Mol. Biol.* 275:677–694.

Mark, A. E., and W. F. van Gunsteren. 1992. Simulation of the thermal denaturation of hen egg white lysozyme: trapping the molten globule state. *Biochemistry.* 31:7745–7748.

Marsh, K. N. 1987. Recommended Reference Materials for the Realization of Physicochemical Properties. Blackwell Scientific Publications, Oxford.

Martì-Renom, M. A., R. H. Stote, E. Querol, F. X. Avilés, and M. Karplus. 1998. Refolding of potato carboxypeptidase inhibitor by molecular dynamics simulation with disulfide bond constraints. *J. Mol. Biol.* 284: 145–172.

Nee, T.-W., and R. Zwanzig. 1970. Theory of dielectric relaxation in polar liquids. *J. Chem. Phys.* 52:6353–6363.

Postma, J. P. M. 1985. MD of H_2O. Ph.D. thesis. Rijksuniversiteit, Groningen, the Netherlands.

Powles, J. G. 1953. Dielectric relaxation and the internal field. *J. Chem. Phys.* 21:633–637.

Ryckaert, J.-P., G. Ciccotti, and H. J. C. Berendsen. 1977. Numerical integration of the Cartesian equations of motion of a system with constraints: molecular dynamics of *n*-alkanes. *J. Comp. Chem.* 23: 327–341.

Schmidt, E. 1989. Zustandsgrössen von Wasser und Wasserdampf in SI-Einheiten (Properties of Water and Steam in SI-Units), 4th Ed. Springer-Verlag, Berlin.

Scott, W. R. P., P. H. Hünenberger, I. G. Tironi, A. E. Mark, S. R. Billeter, J. Fennen, A. Torda, T. Huber, P. Krüger, and W. F. van Gunsteren. 1999. The GROMOS biomolecular simulation program package. *J. Phys. Chem.* 103:3596–3607.

Tironi, I. G., and W. F. van Gunsteren. 1994. A molecular dynamics simulation study of chloroform. *Mol. Phys.* 83:381–403.

van Gunsteren, W. F., S. R. Billeter, A. A. Eising, P. H. Hünenberger, P. Krüger, A. E. Mark, W. R. P. Scott, and I. G. Tironi. 1996. Biomolecular Simulation: The GROMOS96 Manual and User Guide. vdf Hochschulverlag, ETH Zürich, Switzerland.

Vijayakumar, S., S. Vishveshwara, G. Ravishanker, and D. L. Beveridge. 1993. Differential stability of β-sheets and α-helices in β-lactamase: a high temperature molecular dynamics study of unfolding intermediates. *Biophys. J.* 65:2304–2312.

Walrafen, G. E. 1966. Raman spectral studies of the effects of temperature on water and electrolyte solutions. *J. Chem. Phys.* 44:1546–1558.

Watanabe, K., and M. L. Klein. 1989. Effective pair potentials and the properties of water. *Chem. Phys.* 131:157–167.

Weast, R. C., editor. 1976. Handbook of Chemistry and Physics, 56th Ed. CRC Press, Boca Raton, FL.